PHYSICAL REVIEW E **68**, 065603(R) (2003)

Spatial solitons in type II quasiphase-matched slab waveguides

N.-C. Panoiu,[1] D. Mihalache,[2,3] Hongling Rao,[1,*] and R. M. Osgood, Jr.[1]
[1]*Department of Applied Physics and Applied Mathematics, Columbia University, New York, New York 10027, USA*
[2]*Department of Theoretical Physics, Institute of Atomic Physics, P.O. Box MG-6, Bucharest, Romania*
[3]*ICFO-Institut de Ciencies Fotoniques, Universitat Politecnica de Catalunya, 08034 Barcelona, Spain*
(Received 11 June 2003; published 15 December 2003)

The existence and dynamics of one-dimensional spatial solitons formed upon propagation in quasiphase-matched gratings, through three-wave parametric interaction, is analyzed. We study the general case in which the grating exhibits a periodic modulation of both the refractive index and the second-order susceptibility. It is demonstrated that for negative effective wave vector mismatch the induced third-order nonlinearities increase the domain of soliton instability. Finally, the dependence of the efficiency of the second harmonic generation process in the soliton regime, on the parameters of the grating, is discussed.

DOI: 10.1103/PhysRevE.68.065603 PACS number(s): 42.65.Tg, 42.65.Ky, 42.79.−e, 42.65.Sf

There are several techniques for phase matching the interacting waves in a second harmonic generation (SHG) process. Among them, quasiphase-matching (QPM) technique, known since the early days of nonlinear optics [1], consists of compensating the wave vector mismatch through artificial periodic variation of the quadratic nonlinearity coefficient, $\chi^{(2)}$. It offers several important advantages: it uses the highest possible $\chi^{(2)}$ coefficients; it eliminates the spatial walk-off effects; it can use nonbirefringent materials; and phase matching can be achieved at room temperature. QPM has, thus, found important applications in designing all-optical switching devices, high-energy femtosecond laser sources, or in understanding phenomena related to the soliton formation and their propagation in $\chi^{(2)}$ materials. For a review of QPM methods, see Refs. [2–4]. Depending on the number of interacting waves in a SHG process, there exist two types of phase-matching geometries: in the first case, type I phase matching, there are two interacting waves, the fundamental wave (FW) at frequency ω and the second harmonic (SH) at 2ω, orthogonally polarized. Conversely, in the type II geometry, two waves at ω, FW, orthogonally polarized, generate a wave at 2ω, the SH, polarized along either of the two directions of the input waves. The fact that in a type II SHG process the two FWs are orthogonally polarized makes the dynamics of wave evolution very different as compared to the wave dynamics in a type I SHG process, even in the case in which the two FWs are initially identical.

Over the last few years, soliton formation in quadratic media has been the ground of intense research activity, both experimental and theoretical. Thus, in addition to the first experimental verification of soliton existence in a bulk KTP crystal [5] and $LiNbO_3$ slab waveguides [6], the existence and stability of soliton propagation in quadratic media has been demonstrated for various geometries: spatial solitons in slab waveguides [7] or bulk crystals [8–10] and walking solitons in slab waveguides [11] or bulk crystals [12]. Several theoretical studies have been reported on one-dimensional (1D) [13–17] and, recently, two-dimensional [18] spatial soliton propagation in QPM waveguides, in the type I geometry. These studies have shown, among other things, that the periodic modulation of the quadratic nonlinearity induces an artificial cubic nonlinearity that can compete with the former one, a phenomenon that has also been observed experimentally [19]. The first experimental verification of two-dimensional soliton formation in QPM gratings was reported in Ref. [20]. For a comprehensive review on quadratic solitons, see Refs. [21,22].

In this Rapid Communication we present, to our knowledge for the first time, a theoretical analysis of soliton formation and stability upon propagation in planar QPM waveguide gratings, in the type II geometry, by taking into account the higher-order nonlinearities induced by the periodicity of the grating [13]. We consider both gratings for which the average $\chi^{(2)}$ coefficient vanishes [23], as well semiconductor based gratings for which both the average $\chi^{(2)}$ coefficient and the modulation of the refractive indices are different from zero [24,25].

We consider the propagation in a lossless QPM grating, under type II SHG conditions, of two orthogonally polarized cw beams at frequency ω and their SH at frequency 2ω. The QPM grating consists of a periodic structure, for which both the linear part of the susceptibility (refractive index) and the quadratic susceptibility are periodic functions of the longitudinal distance, as it is illustrated in Fig. 1. Under these conditions, expressed in dimensionless units, the dynamics of the three normalized copropagating waves is governed by the following system of equations,

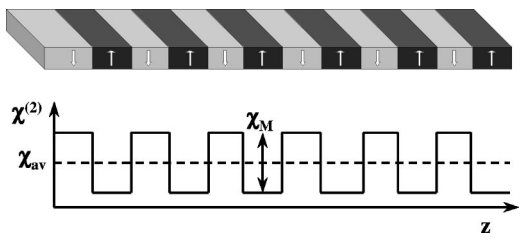

FIG. 1. Schematic presentation of a QPM grating: χ_{av} is the average value of the quadratic nonlinearity, χ_M is its modulation amplitude.

*Present address: RSoft Design Group, 200 Executive Boulevard, Ossining, NY 10562.

$$i\phi_\zeta+\phi_{\tau\tau}+\alpha_\phi(\zeta)\phi+\Gamma(\zeta)\varphi^*\psi e^{-i\beta\zeta}=0,$$

$$i\varphi_\zeta+\varphi_{\tau\tau}+\alpha_\varphi(\zeta)\varphi+\Gamma(\zeta)\phi^*\psi e^{-i\beta\zeta}=0, \qquad (1)$$

$$i\psi_\zeta+\tfrac{1}{2}\psi_{\tau\tau}+\alpha_\psi(\zeta)\psi+\Gamma(\zeta)\phi\varphi e^{i\beta\zeta}=0,$$

where ϕ and φ are the normalized FWs, ψ is the normalized field at SH, ζ and τ are the normalized longitudinal and transversal distances, respectively, and $\beta=z_0(k_\phi+k_\varphi-k_\psi)\equiv z_0\Delta k$ is the normalized wave vector mismatch, with $k_{\phi,\varphi,\psi}$ the corresponding wave vectors. Here, $z_0=k_\psi w_0^2$, with w_0 the characteristic beam width. The normalized coordinates are related to the physical ones, z and x, by the relations $z=z_0\zeta$ and $x=w_0\tau$. The normalized quadratic para-metric interaction coefficient $\Gamma(\zeta)=\omega z_0\chi^{(2)}(z)(2S_0/\epsilon_0c^3\bar{n}_\phi\bar{n}_\varphi\bar{n}_\psi)^{1/2}$, whereas the normalized modulations of the refractive indices are given by $\alpha_{\phi,\varphi}(z)=\omega\Delta n_{\phi,\varphi}(z)/c$ and $\alpha_\psi(z)=2\omega\Delta n_\psi(z)/c$, where $S_0=1\ \mathrm{GW/cm^2}$ is a characteristic beam intensity and $\bar{n}_{\phi,\varphi,\psi}$ and $\Delta n_{\phi,\varphi,\psi}(z)$ are the averages and the modulations of the refractive indices at the corresponding frequency, respectively.

The dynamics of the interacting beams is determined by the interplay among three characteristic lengths. These lengths are the diffraction length z_0, the coherence length $L_c=\pi/|\Delta k|$, and the domain length Λ. In normalized units, $z_0=1$ and $L_c=\pi/|\beta|$. We consider here a typical QPM grating for which the domain length is much smaller than the diffraction length, that is, $\Lambda\ll 1$. Then, the grating wave vector defined by $|\kappa|=\pi/\Lambda$ satisfies the relation $|\kappa|\gg 1$. Under these circumstances, the dynamics of the beam interaction can be described by a set of averaged equations [13]. Following the method introduced in Ref. [13], we expand in Fourier series the grating parameters $\alpha_{\phi,\varphi,\psi}$ and Γ and the fields $\phi(\zeta,\tau)$, $\varphi(\zeta,\tau)$, and $\psi(\zeta,\tau)$:

$$\Gamma(\zeta)=\gamma_0+\gamma\sum_n g_n e^{in\kappa\zeta}, \qquad (2)$$

$$\alpha_{\phi,\varphi,\psi}(\zeta)=a_{\phi,\varphi,\psi}\sum_n g_n e^{in\kappa\zeta}, \qquad (3)$$

$$\phi=\sum_n \phi_n(\zeta,\tau)e^{in\kappa\zeta},\quad \varphi=\sum_n \varphi_n(\zeta,\tau)e^{in\kappa\zeta},$$
$$\psi=\sum_n \psi_n(\zeta,\tau)e^{i(n\kappa+\bar{\beta})\zeta}, \qquad (4)$$

where γ_0 and γ are the average and the modulation amplitude of the parametric coupling strength, respectively, $a_{\phi,\varphi,\psi}$ are the amplitudes of the modulation of the refractive index at the frequencies of the two harmonics, $\phi_n(\zeta,\tau)$, $\varphi_n(\zeta,\tau)$, and $\psi_n(\zeta,\tau)$ are slowly varying functions with respect to ζ and τ, as compared to $e^{i\kappa\zeta}$, and $\bar{\beta}=\beta-\kappa$ is the effective phase mismatch parameter. We assume that the phase mismatch introduced by the QPM grating can be very well controlled, so that $\bar{\beta}$ is very small (although both β and $|\kappa|$ must be large). For the geometry in Fig. 1, the Fourier coefficients $g_n=2\,\mathrm{sgn}(\kappa)/i\pi n$ for n odd and $g_n=0$ otherwise. Here, the $\mathrm{sgn}(\kappa)$ factor ensures that both positive and negative values of κ correspond to the same grating. Consequently, since $\mathrm{sgn}(\beta)=\mathrm{sgn}(\kappa)$, we can treat both cases $\beta\lessgtr 0$ simultaneously.

Furthermore, if one assumes that the higher harmonics in the expansions (4) are of the order $\mathcal{O}(1/|\kappa|)$ or smaller whereas the zero-order ones are of the order $\mathcal{O}(1)$, then, by inserting the expressions (2)–(4) in the system (1) and collecting all terms at the lowest order in $1/|\kappa|$, $\mathcal{O}(1)$, we obtain the relationships between the higher-order Fourier coefficients and the zero-order ones (or, as called in this paper, the average fields)

$$\phi_{n\neq 0}=[a_\phi g_n\phi_0+(\gamma_0\delta_{n,-1}+\gamma g_{n+1})\varphi_0^*\psi_0]/n\kappa,$$

$$\varphi_{n\neq 0}=[a_\varphi g_n\varphi_0+(\gamma_0\delta_{n,-1}+\gamma g_{n+1})\phi_0^*\psi_0]/n\kappa, \qquad (5)$$

$$\psi_{n\neq 0}=[a_\psi g_n\psi_0+(\gamma_0\delta_{n,1}+\gamma g_{n-1})\phi_0\varphi_0]/n\kappa.$$

Then, by inserting these expressions in the system (1) and neglecting higher-order terms in the corresponding system that describes the evolution of the zero-order (average) fields, we end up with the following system of equations that describes the evolution of the zero-order fields

$$iu_\zeta-\beta_u u+u_{\tau\tau}+\sigma v^*w+\delta(|v|^2-|w|^2)u=0,$$

$$iv_\zeta-\beta_v v+v_{\tau\tau}+\sigma u^*w+\delta(|u|^2-|w|^2)v=0, \qquad (6)$$

$$iw_\zeta-\tilde{\beta}w+\tfrac{1}{2}w_{\tau\tau}+\sigma^*uv-\delta(|u|^2+|v|^2)w=0,$$

where $u=\phi_0e^{-i\beta_u\zeta}$, $v=\varphi_0e^{-i\beta_v\zeta}$, $w=\psi_0e^{-i(\beta_u+\beta_v)\zeta}$, and $\tilde{\beta}=\bar{\beta}+\beta_u+\beta_v$ is the residual wave vector mismatch. Here β_u and β_v are the nonlinear wave vector shifts of the FW. The parameters σ and δ are given by the following expressions:

$$\sigma=\frac{2i\,\mathrm{sgn}(\kappa)}{\pi}[\gamma_0(a_\phi+a_\varphi-a_\psi)/\kappa-\gamma], \qquad (7)$$

$$\delta=[\gamma_0^2+\gamma^2(1-8/\pi^2)]/\kappa, \qquad (8)$$

and represent the effective second-order nonlinearity and the induced third-order nonlinearity, respectively. Note that through this procedure one takes into account the influence of all terms in Eqs. (2)–(4) on the average fields; however, this is done only to the order $\mathcal{O}(1/|\kappa|)$. Finally, by introducing the rescaled fields $\bar{u}=|\sigma|u$, $\bar{v}=|\sigma|v$, and $\bar{w}=\sigma w$, the system (6) becomes

$$i\bar{u}_\zeta-\beta_u\bar{u}+\bar{u}_{\tau\tau}+\bar{v}^*\bar{w}+\bar{\delta}(|\bar{v}|^2-|\bar{w}|^2)\bar{u}=0,$$

$$i\bar{v}_\zeta-\beta_v\bar{v}+\bar{v}_{\tau\tau}+\bar{u}^*\bar{w}+\bar{\delta}(|\bar{u}|^2-|\bar{w}|^2)\bar{v}=0, \qquad (9)$$

$$i\bar{w}_\zeta-\tilde{\beta}\bar{w}+\tfrac{1}{2}\bar{w}_{\tau\tau}+\bar{u}\bar{v}-\bar{\delta}(|\bar{u}|^2+|\bar{v}|^2)\bar{w}=0,$$

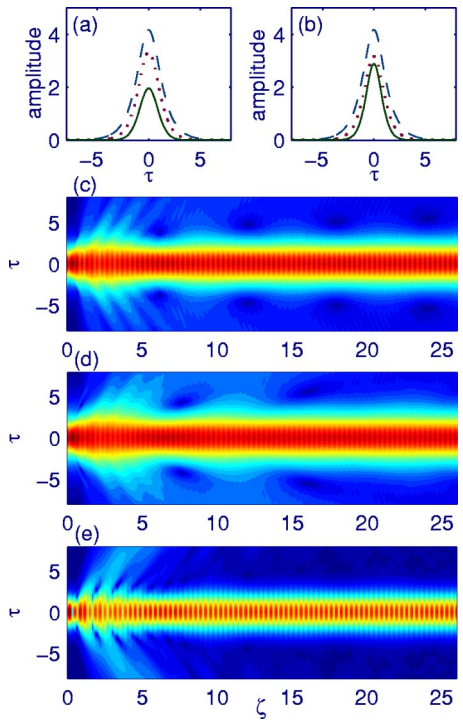

FIG. 2. QPM solitons of the system (9) with parameters $\overline{\beta}=2$, $\beta_u=2$, $\beta_v=1$, and two values of the induced nonlinearity, $\overline{\delta}=0.05$ (a) and $\overline{\delta}=-0.05$ (b). The curves plot the $\overline{u}$ $(\cdots)$, $\overline{v}$ (- - -), and $\overline{w}$ (—) fields along the transverse distance τ. Panels (c), (d), and (e) correspond to the fields $\phi(\zeta,\tau)$, $\varphi(\zeta,\tau)$, and $\psi(\zeta,\tau)$, respectively, for the solitons in (a).

where $\overline{\delta}=\delta/|\sigma|^2$. Note that this analysis can be easily extended to the 2D case.

In order to study the soliton solutions of the system (1) we first determine the soliton solutions (solitary waves) of the system (9), whose coefficients do not depend on the longitudinal distance ζ. Then, the average fields $\{\phi_0,\varphi_0,\psi_0\}$ are determined from the bar fields $\{\overline{u},\overline{v},\overline{w}\}$ and subsequently, from Eqs. (4) and (5), we compute the fields ϕ, φ, and ψ at the input facet of the QPM grating. Finally, these fields are used as initial conditions for the system (1); we then propagate them numerically in the actual QPM grating; and verify whether they reach a regime of stationary propagation, i.e., whether they behave as soliton solutions. The soliton solutions of the system (9) are defined as solutions of the system obtained from (9) by dropping the ζ derivatives, i.e., solutions which are ζ independent. We found these solutions numerically by a standard relaxation method; an example is presented in Fig. 2(a,b), for two values of $\overline{\delta}$. A set of values for the grating parameters that corresponds to these soliton parameters are $a_{\phi,\varphi,\psi}=0$, $\gamma_0=0$, $\gamma=1$, and $\kappa=9.35$. Figure 2 shows that the solitons of the system (9) approximate the solitons of the full system (1) very closely: after a transient propagation distance over which part of the soliton energy is radiated, the beam propagation stabilizes and its profile, at each harmonic, follows the profile of the grating. Thus, the soliton that is formed can be viewed as a beam with its envelope described by the system (9), and whose intensity profile follows the periodicity of the grating.

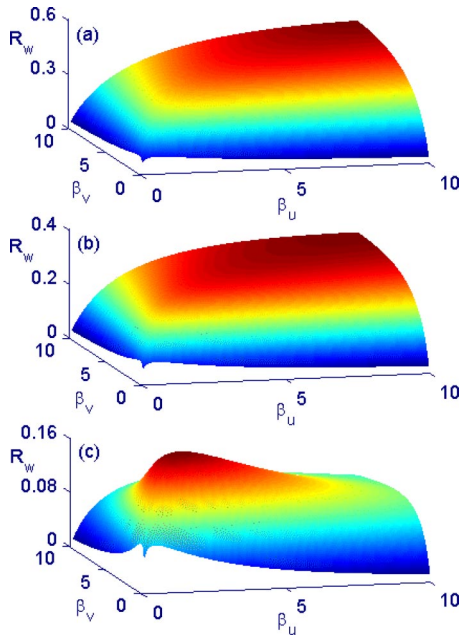

FIG. 3. The fraction $R_w=I_w/I_{tot}$ of the beam intensity at the SH vs the nonlinear wave vectors β_u and β_v, calculated for $\overline{\beta}=2$ and $\overline{\delta}=-0.05$ (a), $\overline{\delta}=0$ (b), and $\overline{\delta}=0.05$ (c).

As seen in Fig. 2(a,b), the induced Kerr nonlinearities have a strong influence on the characteristics of the soliton solutions. To study in more detail this aspect, we determined the dependence on the soliton parameters β_u, β_v, and $\overline{\beta}$ of the total beam intensity I_{tot} and the unbalanced beam intensity I_{unb}. These quantities are constants of motion associated with the system (9) and are given by the following equations:

$$I_{tot}=\int d\tau(|\overline{u}|^2+|\overline{v}|^2+2|\overline{w}|^2)/2, \tag{10}$$

$$I_{unb}=\int d\tau(|\overline{u}|^2-|\overline{v}|^2)/2, \tag{11}$$

In Fig. 3 we show the fraction $R_w=I_w/I_{tot}$ of the beam intensity at the SH, calculated for $\overline{\beta}=2$, for three values of the induced third-order nonlinearity coefficient $\overline{\delta}$. This figure shows that, as $\overline{\delta}$ increases, the fraction R_w of the SH decreases and, for a fixed $\overline{\delta}$, it increases with nonlinear wave vectors β_u and β_v. Interestingly, for $\overline{\delta}>0$ there is a certain value of the parameters β_u and β_v for which R_w reaches a maximum. For instance, at $\overline{\beta}=2$, for $\overline{\delta}=0.05$ the ratio R_w is maximum at $\beta_u^0=\beta_v^0=1.65$.

Finally, in what follows we discuss the influence of the Kerr-induced nonlinearity on the stability properties of the QPM solitons. To begin with, we mention that the system (9) has soliton solutions only if $\beta_{u,v}>0$ and $\tilde{\beta}>0$, i.e., $\beta_u+\beta_v>-\overline{\beta}$. Therefore, for $\overline{\beta}>0$ solitons exist for positive $\beta_{u,v}$ whereas for $\overline{\beta}<0$ solitons exist for $\beta_u+\beta_v>|\overline{\beta}|$. Fur-

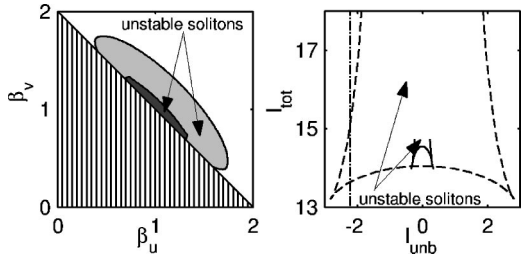

FIG. 4. Left, soliton stability domains determined for $\bar{\beta}=-2$ and $\bar{\delta}=0.15$ (dark gray) and $\bar{\delta}=0.3$ (light gray). Right, the same stability domains represented in $(I_{\mathrm{unb}},I_{\mathrm{tot}})$ plane: $\bar{\delta}=0.15$ (—) and $\bar{\delta}=0.3$ (- - -).

thermore, the boundary of the domain of stable solitons is given by the following equation [26]:

$$\frac{\partial(I_{tot},I_{unb})}{\partial(\beta_u,\beta_v)}=0. \tag{12}$$

We determined the stability domains numerically and summarize the results as follows. For $\bar{\beta}>0$ solitons are stable, for all physically meaningful values of $\bar{\delta}$, namely $\bar{\delta}\lesssim 0.5$. In contrast, for $\bar{\beta}<0$, solitons are unstable within a certain domain, whose size increases with $\bar{\delta}$. These results are summarized by Fig. 4. This figure illustrates another important phenomenon, namely, *multistability* of solitons of system (9). Thus, if the stability domains are represented in the $(I_{\mathrm{unb}},I_{\mathrm{tot}})$ plane (see right panel in Fig. 4), one sees that for certain fixed values of I_{unb} there are two stable branches of stable solutions. Therefore, it is possible that at the same values of invariants I_{tot} and I_{unb} correspond two stable solutions [27]. Furthermore, as the difference ΔI_{tot} between the crossing points increases with $\bar{\delta}$, one expects that the quality of this multistability, as introduced in [28], is enhanced by the induced Kerr nonlinearity; however, a quantitative description of this phenomenon is beyond the scope of this paper. To investigate whether these stability properties of the solitons of the averaged system (9) can be extended to solitons of the full system (1), we performed an extensive series of numerical simulations. Thus, solitons corresponding to different regions in the parameter space in Fig. 4 were used as initial conditions for system (1). With these initial conditions, the system (1) was then numerically integrated. The conclusion of these numerical tests was that, for $\bar{\delta}\lesssim 0.5$, stable solitons that correspond to system (9) remain stable upon propagation in the grating described by the full system (1). More exactly, when propagated in the actual grating, stable solitons of system (9) showed oscillations that followed the periodicity of the grating, but their envelope remained stable.

In conclusion, we have determined the characteristics of 1D-soliton formation and their stability upon propagation in a QPM grating, for the type II geometry. It has been demonstrated that at the first order of a perturbation theory the soliton propagation in the QPM grating is strongly influenced by the induced focusing or defocusing Kerr-type nonlinearities. Finally, the influence of this induced Kerr nonlinearity on the stability properties of the QPM solitons has been analyzed and the theoretical results were verified by systematic numerical simulations.

This work has been supported by the NIST Advanced Technology Program Cooperative Agreement, Grant No. 70NANB8H4018.

[1] J.A. Armstrong *et al.*, Phys. Rev. **127**, 1918 (1962).
[2] M.M. Fejer *et al.*, IEEE J. Quantum Electron. **28**, 2631 (1992).
[3] M. Houe and P.D. Townsend, J. Phys. D **28**, 1747 (1995).
[4] L.E. Myers *et al.*, J. Opt. Soc. Am. B **12**, 2102 (1995).
[5] W.E. Torruellas *et al.*, Phys. Rev. Lett. **74**, 5036 (1995).
[6] R. Schiek, Y. Baek, and G.I. Stegeman, Phys. Rev. E **53**, 1138 (1996).
[7] A.V. Buryak and Y.S. Kivshar, Opt. Lett. **19**, 1612 (1994); D.E. Pelinovsky, A.V. Buryak, and Y.S. Kivshar, Phys. Rev. Lett. **75**, 591 (1995); L. Torner *et al.*, Opt. Lett. **20**, 2183 (1995).
[8] L. Torner *et al.*, Opt. Commun. **121**, 149 (1995).
[9] L. Berge *et al.*, Phys. Rev. A **52**, R28 (1995); Phys. Rev. E **55**, 3555 (1997).
[10] O. Bang *et al.*, Phys. Rev. E **58**, 5057 (1998).
[11] L. Torner, D. Mazilu, and D. Mihalache, Phys. Rev. Lett. **77**, 2455 (1996).
[12] D. Mihalache *et al.*, Opt. Commun. **137**, 113 (1997).
[13] C.B. Clausen, O. Bang, and Y.S. Kivshar, Phys. Rev. Lett. **78**, 4749 (1997); J.F. Corney and O. Bang, *ibid.* **87**, 133901 (2001); Phys. Rev. E **64**, 047601 (2001).
[14] C.B. Clausen *et al.*, Phys. Rev. Lett. **83**, 4740 (1999).
[15] O. Bang and J.F. Corney, Opt. Photonics News **12**, 42 (2001); J.F. Corney and O. Bang, J. Opt. Soc. Am. B **19**, 812 (2002).
[16] O. Bang *et al.*, Opt. Lett. **24**, 1413 (1999).
[17] A. Kobyakov *et al.*, Opt. Lett. **23**, 506 (1998); O. Bang, T.W. Graversen, and J.F. Corney, *ibid.* **26**, 1007 (2001).
[18] N.C. Panoiu *et al.*, Phys. Rev. E **68**, 016608 (2003).
[19] P. Di Trapani *et al.*, Phys. Rev. Lett. **87**, 183902 (2001).
[20] B. Bourliaguet *et al.*, Opt. Lett. **24**, 1410 (1999); H. Kim *et al.*, *ibid.* **28**, 640 (2003).
[21] C. Etrich *et al.*, in *Progress in Optics*, edited by E. Wolf (North Holland, Amsterdam, 2000), Vol. 41, pp. 483–568.
[22] A.V. Buryak *et al.*, Phys. Rep. **370**, 63 (2002).
[23] A.M. Radojevic *et al.*, Opt. Lett. **25**, 1034 (2000).
[24] S.J. Yoo *et al.*, Appl. Phys. Lett. **66**, 3410 (1995).
[25] A. Fiore *et al.*, Appl. Phys. Lett. **72**, 2942 (1998).
[26] A.V. Buryak, Y.S. Kivshar, and S. Trillo, Phys. Rev. Lett. **77**, 5210 (1996).
[27] A.V. Buryak and Y.S. Kivshar, Phys. Rev. Lett. **78**, 3286 (1997).
[28] I. Towers *et al.*, J. Opt. Soc. Am. B **17**, 2018 (2000).